Geophysical Journal International

Geophys. J. Int. (2014) **199,** 1278–1285 doi: 10.1093/gji/ggu317
GJI Seismology

Intensity-distance attenuation laws for the Portugal mainland using intensity data points

Boris Le Goff, José Fernando Borges and Mourad Bezzeghoud

Departamento de Física and Centro de Geofísica de Évora, Escola de Ciências e Tecnologia, Universidade de Évora, Rua Romão Ramalho, 59, 7002-554 *Évora, Portugal. E-mail:* earthscream@gmail.com

Accepted 2014 August 13. Received 2014 August 12; in original form 2014 February 20

SUMMARY

In this study, new intensity-distance attenuation law is presented, using directly the intensity observations, rather than the subjective, and sometimes controversial, isoseismal lines. This intensity-distance attenuation law is the only one defined for Portugal mainland, which is expressed as a function of magnitude. We computed this attenuation law using the slope and the intercept of the logarithmic regression of 25 events, with magnitudes between 4.4 and 6.2.

Using the Bakun and Wentworth method (1997), this new attenuation law allows performing better results in the earthquake epicentral position and magnitude estimations of the 1909 Benavente event than the Atkinston and Boore attenuation law (1997). This law also gives good results in the study of site effects, presenting good matches between intensity residuals and geological structures where site effects are expected.

Key words: Earthquake ground motions; Earthquake source observations; Seismicity and tectonics; Seismic attenuation; Site effects.

1 INTRODUCTION

In low to moderate seismic regions, like the continental part of Portugal, the computation of attenuation laws is made difficult by the lack of data. Given that most of the largest earthquakes occurred before the development of seismic instruments, the instrumental data are small and are related to low magnitude events.

The attenuation laws are mainly used to compute the seismic hazard. Usually, in regions of moderate tectonic and seismic activity, such as the study area, the resulting seismic hazard is computed using pre-existing attenuation laws, developed for similar areas and for similar ranges of magnitude. In Portugal, Vilanova & Fonseca (2007) computed the probabilistic seismic hazard using three attenuation models (included into a logic tree): Ambraseys *et al.* (1996), Toro *et al.* (1997) and Atkinson & Boore (1997), developed for target areas of Europe and Middle-East in one case and Central and Eastern North America on the other two.

Several attempts have been done to evaluate an attenuation law in the Iberian Peninsula (Muñoz 1974; Martín 1984; Lopez Casado *et al.* 1992; Sousa & Oliveira 1997; Lopez Casado *et al.* 2000). Yet, the results do not directly use the intensity data points of the available events but the isoseismal maps instead. These isoseismal lines are set by expert decisions, introducing a subjective part into the resulting laws. The main advantage of using directly the intensity data points is that the procedures are explicit so that the results are reproducible. Moreover, in most of the studies, the attenuation laws are not expressed as a function of the magnitude, but as a function of the epicentral intensity I_0.

We developed a new intensity-distance attenuation law for the continental Portugal, using the macroseismic reports of events that provide intensity data points and instrumental magnitudes. This law is directly derived from the intensity data points and expressed as a function of magnitude and epicentral distance.

The methodology includes three steps: (1) the estimation of the equation form, (2) the study of the attenuation law parameters as a function of the magnitude and (3) the definition of the attenuation equation. The attenuation law will be provided with its associated uncertainties. It is important to notice that the obtained attenuation law does not take into account the site effects.

Subsequently, two methods are achieved using the new intensity-distance attenuation law to validate it. The first one consists in relocating the Benavente earthquake occurred the 1909 April 23 (moment magnitude $M_w = 6$), located closed to Lisbon, with the Bakun and Wentworth method (1997), using (1) the Atkinson & Boore (1997) attenuation law (used in the Portuguese PSHA calculation) and (2) the new attenuation law, in order to validate whether the use of the new attenuation law improves the results. The second one consists in studying the site effects and check if there is a correlation between them and the intensity residuals, defined by the difference between the observed 1909 Benavente event intensity data points and the ones calculated with the new attenuation law, into which the site effects are not expressed.

2 DATA

The data required for the computation of the attenuation law, have to provide an instrumental magnitude and a felt intensity report. We obtained, from the Instituto Português do Mar e da Atmosfera (IPMA, Portugal; ex-IM), 30 events, covering the period since 1909 until 1997. These events are listed in the Table 1 and mapped in the Fig. 1. The largest magnitude is $M_s = 8.4$ for the 1941 November 25 earthquake, located closed to the boundary separating the Eurasian and the Nubian plates. The intensities are expressed in the Modified Mercalli scale. The magnitudes are expressed in different scales and are converted to a homogeneous magnitude. The moment magnitude, M_w, is chosen as reference. The magnitudes provided by the Instituto Geografico Nacional (IGN, Madrid) are calculated in m_{bLg}. The ones collected from publications (Buforn *et al.* 1988a,b, 1995; Grandin *et al.* 2007) are expressed as surface wave magnitude, M_s. We noticed that the magnitudes (m_b) provided by the IPMA are equals to the ones calculated by the IGN. So, we consider $m_b = m_{bLg}$ for the conversions. The relations of Johnston (1996a) are chosen for the conversions. These empirical relationships are used to convert both teleseismic (M_s and M_L) and regional magnitudes to M_0 (dyn cm) for stable continental crust earthquakes. The relationships are the followings:

$$\log M_0 = 24.66 - 1.083 M_s + 0.192 M_s^2 \quad \text{for} \quad M_s \geq 3.6 \qquad (1)$$

$$\log M_0 = 18.28 + 0.679\, m_b + 0.077\, m_b^2. \qquad (2)$$

Due to the small number of observed intensities (only 4), the 1909 December 8 and the 1912 January 23 earthquakes are not considered in this study.

For this study, the 1909 Benavente event will be considered as a reference because it is the most documented, owing to the preliminary work of Bensaúde (1910) and the work of macroseismic field revision of Teves-Costa & Batlló (2011).

Here we only use epicentral distances because large uncertainties on the earthquake depths or the lack of value prevent to consider hypocentral distances. The definition of epicentral distances is essential. The intensity data point refers to a municipality and the location of this intensity data point is situated in the city centre or city hall of this municipality. This may lead to an uncertainty in the calculation of the epicentral distance that depends on the municipality density. An area with a lot of municipalities will have more accurate intensity data point locations than an isolated municipality. The quality of the intensity data point itself is also controlled by this municipality density but also by the population density. Indeed, an isolated building located on a sedimentary basin, may suffer more important damage than the closest city, where this intensity observation will be associated. Moreover, the intensity data point for this city will be the one based on the damage statement of one isolated building or the testimony of the few people living there.

3 METHODOLOGY

The methodology used to compute the attenuation law for the Portugal mainland is inspired from Bakun & Wentworth (1997). First we need to estimate the equation form. It consists in defining for each event the regression line that better fits the intensity data points as a function of the epicentral distances. We consider here the median epicentral distance for each range of intensity to

Table 1. Seismic events used to estimate the attenuation law. IPMA, Instituto Português do Mar e da Atmosfera; ISC, International Seismological Center; IGN, Instituto Geografico Nacional.

Date	Latitude (°)	Longitude (°)	Magnitude	Type of M	Source	M_w	Number of intensities	ID
23/04/1909	38.9	−8.8	6	M_w	Teves-Costa & Batlló (2011)	**6.0**	504	1
04/05/1909	38.9	−8.8	4.5	m_b	IPMA	**4.6**	20	2
11/06/1909	38.9	−8.8	5	m_b	IPMA	**5.0**	14	3
17/08/1909	38.9	−8.8	5.19	m_b	IPMA	**5.2**	17	4
08/12/1909	38.9	−8.8	5.19	m_b	IPMA	**5.2**	4	5
09/02/1911	41.7	−8.9	5	m_b	IPMA	**5.0**	7	6
12/08/1911	36.5	−7.8	4.8	m_b	IPMA	**4.8**	17	7
23/01/1912	38.8	−7.8	5	m_b	IPMA	**5.0**	4	8
11/07/1912	36.5	−7.8	5	m_b	IPMA	**5.0**	18	9
18/10/1912	41.5	−8.5	5	m_b	IPMA	**5.0**	36	10
27/10/1913	41.67	−8.72	5	m_b	IPMA	**5.0**	18	11
23/09/1914	38.9	−8.8	5.3	m_b	IPMA	**5.3**	12	12
25/09/1914	38.9	−8.8	5.3	m_b	IPMA	**5.3**	83	13
11/07/1915	37	−10.5	6.2	M_s	ISC	**6.3**	71	14
02/03/1924	38.9	−8.8	5	m_b	IPMA	**5.0**	17	15
28/02/1926	38.5	−8	5.5	m_b	IPMA	**5.5**	104	16
10/02/1930	37.4	−8.1	5	m_b	IPMA	**5.0**	38	17
25/11/1941	37.5	−18.5	8.4	M_s	Buforn *et al.* (1988)	**8.7**	61	18
27/12/1941	36	−10.5	6.8	M_s	ISC	**6.7**	16	19
02/10/1947	38.5	−9.9	5.1	m_b	IPMA	**5.1**	47	20
12/08/1948	40.1	−8.6	5.2	m_b	IPMA	**5.2**	33	21
05/12/1960	35.6	−7.2	5	m_b	IPMA	**5.0**	7	22
10/02/1961	41.51	−6.02	5.2	m_b	IPMA	**5.2**	14	23
15/03/1964	36.09	−7.86	6.2	M_s	Buforn *et al.* (1995)	**6.2**	81	24
28/02/1969	35.94	−10.85	8	M_s	Grandin *et al.* (2007)	**8.2**	194	25
24/12/1969	36	−10	5	m_b	ISC	**5.0**	7	26
14/06/1972	36.7	−8.4	5.2	m_{bLg}	IGN	**5.2**	20	27
04/04/1982	39	−10.3	4.4	m_{bLg}	IGN	**4.5**	16	28
10/08/1986	41.03	−7.16	4.3	m_{bLg}	IGN	**4.4**	41	29
21/05/1997	42.43	−7.17	5.2	m_b	ISC	**5.2**	72	30

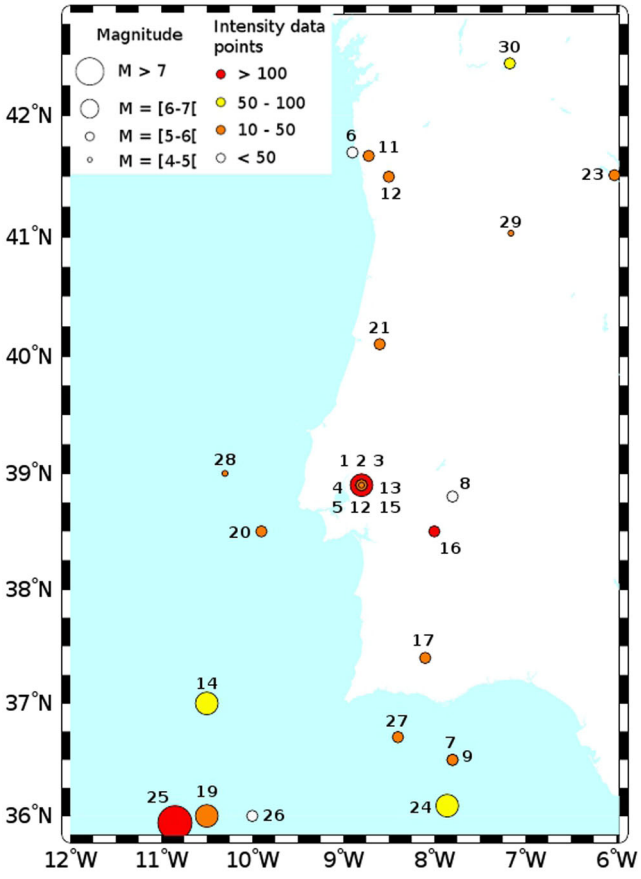

Figure 1. Map of the seismic events used to estimate the attenuation law (the 1941 earthquake of $M_s = 8.4$ is out of this map). Numbers in the map correspond to the ID of the earthquake (see Table 1)

minimize the weight of extreme values, which might be erroneous or exaggerated. Three different kinds of regression are tested: linear, exponential and logarithmic. For each event, the regression coefficient of the different tendencies is calculated and compared each other. The tendency that presents the best regression coefficients over all events is used to define the form of the attenuation equation.

Once we obtained the form of the attenuation equation, we study the behaviour of its parameters as a function of the magnitude. These parameters correspond to the slope and the intercept of the attenuation law. The slope of the logarithmic regression of each earthquake is represented as a function of its corresponding magnitude. Then, the evolution of the slope with the magnitude is estimated. Similar plot is obtained using the intercepts instead of the slopes, to evaluate the behaviour of these intercepts with the magnitude. This allows defining the analytic form of the different parameters that are introduced into the attenuation equation.

Finally, from the complete analytic expression of the attenuation equation, the attenuation law is obtained using a weighted least-square method. This method provides the uncertainty associated to the attenuation law.

Then, we tested our attenuation law by relocating the 1909 Benavente event with the Bakun and Wentworth method (1997) and by comparing the results with a relocation using the Atkinson & Boore (1997) attenuation law. We expect a better earthquake epicentral position with the law developed in this study.

We also tested our attenuation law by studying the site effects. Because our attenuation law does not include site effects, the positive intensity residuals (that is the difference between the observed and theoretical intensities: $I_{obs} - I_{theo}$) should match with Portuguese regions where site effects are known (Bezzeghoud *et al.* 2011), like the Meso-Cenozoic basins.

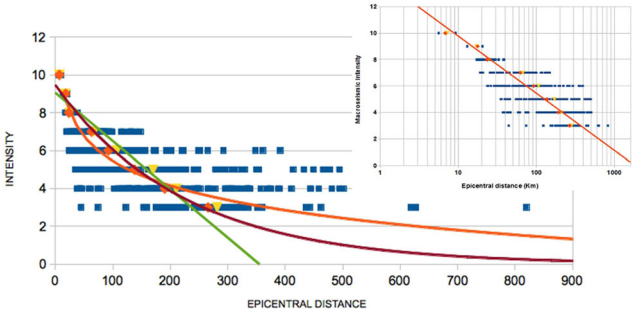

Figure 2. Intensity data versus Epicentral distance of the 1909 Benavente event. Blue dots represent intensity data. Yellow triangles and orange diamonds represent, respectively, the mean and median epicentral distance for each intensity range. The green, red and orange curves are, respectively, the linear, exponential and logarithmic regressions of the median epicentral distances. Plot in the top-right corner shows the best fit line of the logarithmic regression for the 1909 Benavente observed intensities.

4 RESULTS

4.1 Equation form

In order to estimate the form of the attenuation law, several plots representing the intensity data points versus the epicentral distances, have been achieved for every earthquake. Different regression curves (linear, logarithmic and exponential) have been calculated to identify which one best fit the data (Fig. 2). This regression is achieved for the median epicentral distance of every intensity range, to avoid giving an important weight to the extreme values that might be erroneous or exaggerated.

Considering the regression coefficient, we obtained a mean value of 0.682 for the linear regressions, 0.693 for the exponential ones and 0.710 for the logarithmic ones. According to these regression coefficients, the logarithmic regressions better fit the data, and are used to define the equation form.

This leads to an attenuation equation of the following form:

$$I = C_0(M_w)\ln(D) + C_1(M_w), \quad (3)$$

where I represents the intensity data point, M the magnitude and D the epicentral distance. C_0 and C_1 are the slope and the intercept of the attenuation curve, respectively. So far, we do not know their dependency with the magnitude.

4.2 Behaviour of the parameters C_0 and C_1 related to the magnitude

To estimate the magnitude dependence of C_0, the slope of the logarithmic regression of each earthquake is plotted as a function of its related magnitude (Fig. 3). Note that the median slope is considered for same magnitude events. We observed that the slopes are constant for magnitude lower than 6.2 and seem to decrease for higher magnitudes. The same behaviour is observed in Fig. 4, representing the intercepts of the logarithmic regression of each earthquake versus its related magnitude. The intercepts increase linearly for $M \leq 6.2$ and, increase with different coefficients for larger. If the constant slope and the linear increase of the intercepts for the $M < 6.2$ events

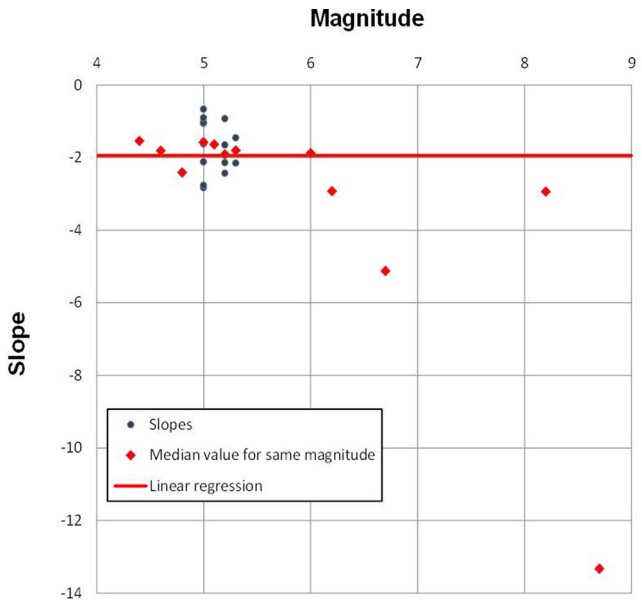

Figure 3. Slopes of the logarithmic regressions versus the magnitudes. The linear regression has been done using events of $M \leq 6.2$.

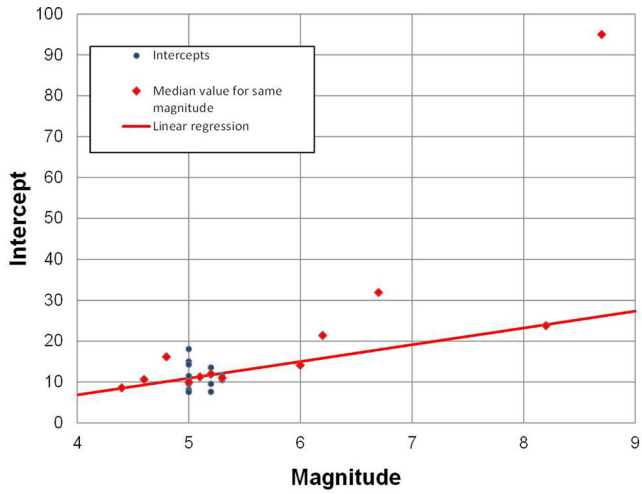

Figure 4. Intercepts of the logarithmic regressions versus the magnitudes. The linear regression has been done using events of $M \leq 6.2$.

are obvious, the linear trend of the decreasing slope and the increasing intercept, for $M \geq 6.2$, are not evident. This is due to the small number of events of $M \geq 6$, and to the lack of intensity data points of small epicentral distances, introducing large uncertainties in the calculation of both slope and intercept. We decided to restrain the attenuation law to the magnitude interval [4.4–6.2].

Constant slope and linear increase of intercepts lead to the following expressions of C_0 and C_1:

$$C_0(M_w) = C_0 \tag{4}$$

and

$$C_1(M_w) = k_1 M_w + k_2. \tag{5}$$

The k_1 and k_2 parameters correspond, respectively, to the slope and the intercept of the linear regression between the intercepts and the magnitudes (Fig. 4).

4.3 Attenuation laws

From the equation form and the expressions of its parameters, we can define the attenuation law.

The attenuation law is expressed as follow:

$$I = C_0 \ln(D) + k_1 M_w + k_2. \tag{6}$$

Using a weighted least-square fit we obtain the following expression:

$$I = -1.9438 \ln(D) + 4.1 M_w - 9.5763. \tag{7}$$

The standard deviation of the residuals is obtained comparing the obtained intensities from the previous attenuation relation with the observed intensities. We obtained a rms standard error of 0.63. Concerning the parameters, the rms are 0.37, 1.19 and 5.69 for the C_0, k_1 and k_2, respectively. The attenuation law is represented with all the data of $M \leq 6.2$ events in the Fig. 5, plotted for the magnitude 4.5, 5.0, 5.5 and 6.0.

The comparison between the observed and the theoretical intensities are expressed in the Fig. 6. We observed that the attenuation laws tends to underestimated the intensities lower than 5 and to overestimate the intensities larger than 5.

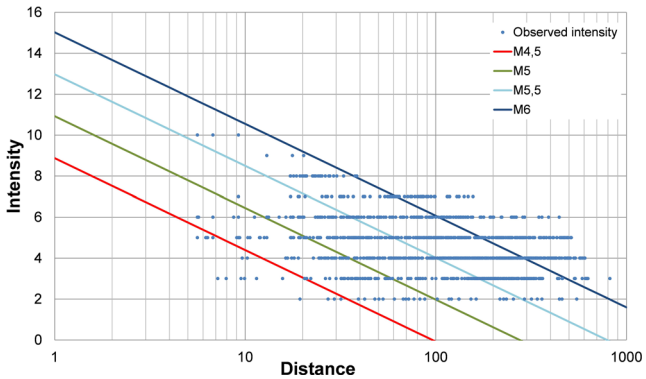

Figure 5. attenuation law plotted for $M = 4.5$, $M = 5.0$, $M = 5.5$ and $M = 6.0$.

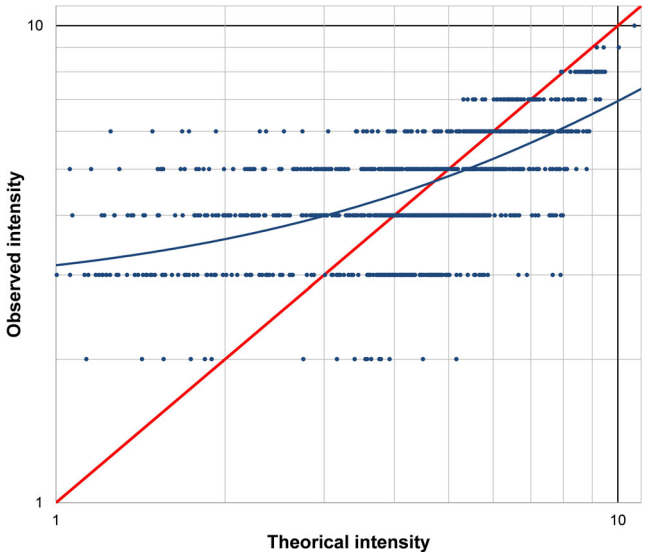

Figure 6. Observed intensity versus theoretical intensity, obtained from the attenuation law. Red line represented the 1:1 trend line. Blue line represents the best-fitting line.

5 VALIDATION

5.1 Relocation using the Bakun and Wentworth methodology (1997)

The methodology of Bakun & Wentworth (1997) allows estimating the epicentral region and the moment magnitude of an earthquake, from its intensity data points. The method consists in defining a magnitude M_I and its related error (noted rms[M_I]) over a grid of assumed epicentres. M_I corresponds to the mean of the M_i, where M_i is the magnitude calculated from the attenuation law related to the ith intensity data point. The rms[M_I] is defined by rms[M_I] = rms($M_I - M_i$) – rms$_0$($M_I - M_i$), where rms is the root mean square and rms$_0$($M_I - M_i$) is the minimum of rms over the grid of assumed epicentres. For each point of this grid, a value of M_I and rms[M_I] is calculated. The epicentral region is bounded by contours of rms[M_I], while the estimated magnitude is bounded by the M_I values. These empirical contour values are estimated for different levels of confidence, associated to the quantity of intensity data points available. This method is particularly appropriate for the evaluation of historical earthquakes, for which the only available data are sparse set of intensity observations.

The earthquake of Benavente occurred the 1909 April 23, in the region of the Lower Tagus Valley. This earthquake is associated to the city of Benavente because it was the city the most damaged.

According to the estimation of Choffat & Bensaude (1912), around 40 per cent of the building collapsed or had to be demolished and another 40 per cent required major repairs. This earthquake is considered as the largest crustal earthquake in the Portugal mainland.

This event is located in the Low Tagus Valley, where severe earthquakes already occurred (1344, 1531), and is associated to the fault system of the Low Tagus Valley (Cabral *et al.* 2000, 2004). The epicentre location was estimated at 38.9°N, 8.8°W, using the available macroseismic information, by Kárník (1969). From different studies, based on the seismic moment estimation, the moment magnitude, *M*w, was estimated between 6.0 and 6.2 and *M*s close to 6.3 (Teves-Costa *et al.* 1999, 2005; Dineva *et al.* 2002; Stich *et al.* 2005).

Stich *et al.* (2005) determined a focal mechanism of a reverse faulting. This is in agreement with other focal mechanisms calculated for this region (Borges *et al.* 2001). However, this focal mechanism is not well constrained due to the lack of data.

Several authors have proposed an isoseismal map for this event (Mezcua 1982; Moreira 1991; Senos *et al.* 1994; Teves-Costa & Batlló 2011). They underline an east–west extension of the isoseismal curves. This extension may be explained by local site effects or by cascading events.

This event is the most documented, owing to the preliminary work of Bensaúde (1910) and the work of macroseismic field revision of Teves-Costa & Batlló (2011) and because of its occurrence in the continent.

Using the attenuation law developed in this study, we re-estimated the epicentral region and the magnitude of the 1909 Benavente event with the Bakun and Wentworth method (1997). The resulting map is presented in the Fig. 7 with the previous results obtained using the Atkinson & Boore (1997) attenuation law.

First, we observe that we obtained a magnitude estimation of $M = 6.1$ (Fig. 7, right-hand side). This is slightly larger than the instrumental magnitude ($M_w = 6.0$), but better than the estimation done with the Atkinson & Boore (1997) law. We also notice that the Kárník (1969) estimation is still within all the confidence level contours.

The minimum of rms[M_I] is getting closer to the Kárník (1969) estimation and the confidence level contours become closers. The N–W extension, presented in the first resulting map (Fig. 7, left-hand side), disappeared.

From these results, we can conclude that the use of the computed attenuation law, appropriate for this region, allows performing better resulting maps of earthquake epicentral position and magnitude estimations. The significant improvement, using this attenuation law, is the estimation of the magnitude that is close to the instrumental one, while the one defined with the Atkinson & Boore (1997) attenuation law underestimates it (Fig. 7, left side). We also observe a

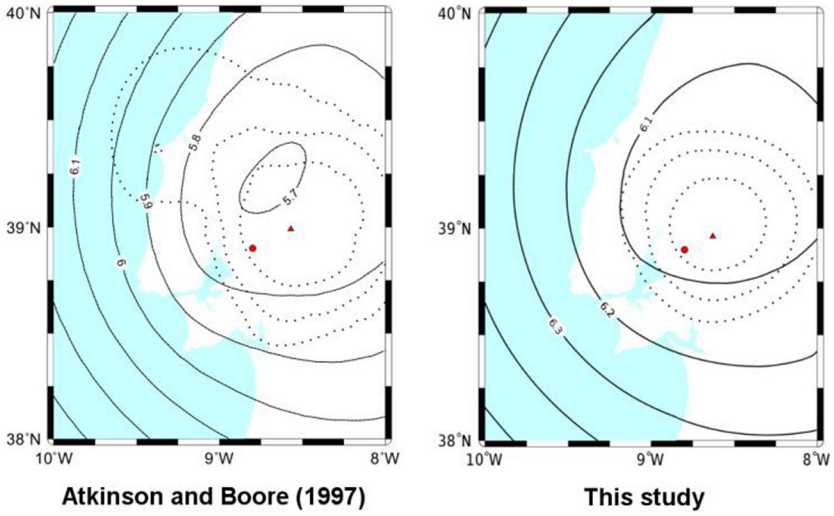

Figure 7. Resulting magnitude and earthquake epicentral position of the 1909 Benavente event, using the Bakun and Wentworth method (1997) with the Atkinson & Boore (1997) attenuation law (left-hand side) and the attenuation law computed in this study (right side). Solid lines represent the contours of *M*. The red dot represents the epicentre estimated by Kárník (1969). The red triangle represents the location of the minimum value of rms[M_I] over a grid of assumed epicentres. The rms[M_I] contours corresponding to the 50, 80 and 95 per cent confidence levels for location are shown as the innermost, middle and outermost contours of the dotted lines, respectively.

better earthquake location with a tightening of the confidence level contours and a minimum of rms[M_l] coming closer to the epicentre estimation of Kárník (1969).

5.2 Site effects

The computed attenuation law does not incorporate site corrections and site effects are not taken into account. By calculating the intensity residuals, ΔI, expressed as the difference between the observed intensities (I_{obs}) and the intensities calculated from the attenuation law (I_{theo}), we can study where they are situated and if they can be correlated with geological structures that present site effects. A positive value of ΔI expresses an underestimation of the theoretical value of the intensity I_{theo}, in regards to the observation value I_{obs}, explained by an amplification. These intensity residuals may be represented through a geographic information system (GIS) with a map of the geological structures. The intensity residuals are then correlated to the topographic slope. Site effects are expected where the topographic slope is low.

We use this methodology with the 1909 Benavente event, which presents a large number of intensity data points with small epicentral distances (0–200 km). The intensity residuals are interpolated and are represented in a GIS (QGIS) with the main basins of Portugal (Fig. 8). We expect positive values of the intensity residuals in the basins, expressing an effect of amplification. The study of Bezzeghoud *et al.* (2011) shows that the Portuguese Meso-Cenozoic basins (Lusitanian basin, Low Tagus basin, Arrabida basin and Algarve basin) are plausible regions for site effects.

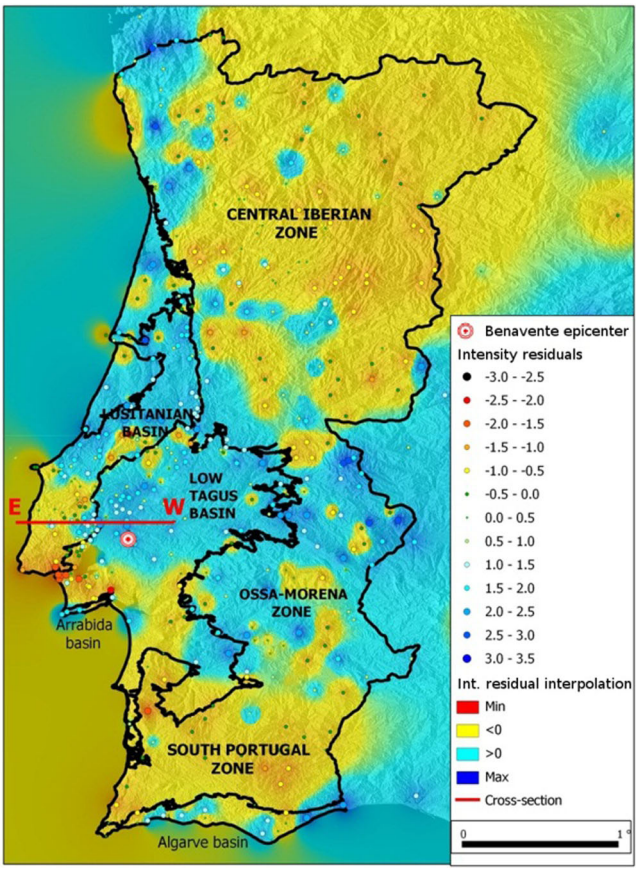

Figure 8. Intensity residuals map and their interpolation.

The northern part of Portugal presents mainly negative intensity residuals, with few positive ones near the ocean. In the central part, the intensity residuals are mainly positives. Some negative values are located in the occidental part of Lisbon, with low punctual residuals around the Tagus river mouth. The southern part is clearly dominated by negative intensity residual values, except some positive values detected in the region of Algarve.

From the intensity residual interpolation map, we may clearly delimitate the different geological structures. The positive values match well with the limits of the Meso-Cenozoic basins, where site effects were already highlighted. We can also isolate the south Portuguese zone and the central Iberian zone, where the intensity residuals are negatives, from the Ossa-Morena zone where intensity residuals are positives. In the south Portuguese zone and in the Central Iberian Zone the negative intensity residuals are best explained by the bedrock made of consolidated rocks (mainly granites). No explanations may explain the positive values of the Ossa-Morena zone as this zone is also mainly composed of granites and should present negatives intensity residuals, because of the high velocity of the seismic wave propagation. The Algarve basin is evidenced by positive values. Even if no limits can be made up between the Lusitanian basin and the Low Tagus basin, both of them can be extracted from the other formations. In spite of the few data in the Arrabida basin, it is possible to differentiate this basin from the Low Tagus basin. The large negative residual values detected around the Tagus river mouth highlight the volcanic complex of Lisbon. Indeed, the fast propagation of seismic waves into volcanic rocks leads to negative intensity residual values. The negative residuals observed in the northwest of Lisbon may be explained by the presence of relief, limiting the rule of the geologic site effects. Unfortunately the lack of data in Spain prevents the intensity residual interpolation map to be interpreted.

A cross-section has been achieved and is represented in the Fig. 9. The part of the graphic with low elevation and low topographic slope corresponds to the Low Tagus basin. We observe a connection between the elevation and topographic slope with the intensity residuals. Positive values are found at the level of the basin, while negative values are observed in the part with higher elevation and slope. This confirms the correlation of the positive intensity residuals with the site effects in the Meso-Cenozoic basins. Nevertheless, we observe another patch of positive intensity residuals, between the kilometres 35 and 45 of the cross-section. Even if few of these intensity residuals may be explained by the intensity location problem, this concentration of positive residuals may be related to the basin edge effect (Choi *et al.* 2005; Paolucci & Morstabilini 2006) or by a transition zone (change of rock composition).

6 DISCUSSION

As mentioned before, the data used to compute the attenuation laws are few and, sometimes, of poor quality. Indeed, only three earthquakes of $M \geq 6.2$ have been collected, without any event intensity data point of epicentral distances lower than 200 km. This lack of nearby intensity data is explained by the offshore location of largest earthquakes. Because of the offshore position of these events, the uncertainties related to their location and their magnitude calculations are considerable.

The attenuation law needs to be updated when new data are available.

The intensity data estimation also contributes to the uncertainty in the attenuation law contribution. Indeed, as explained before,

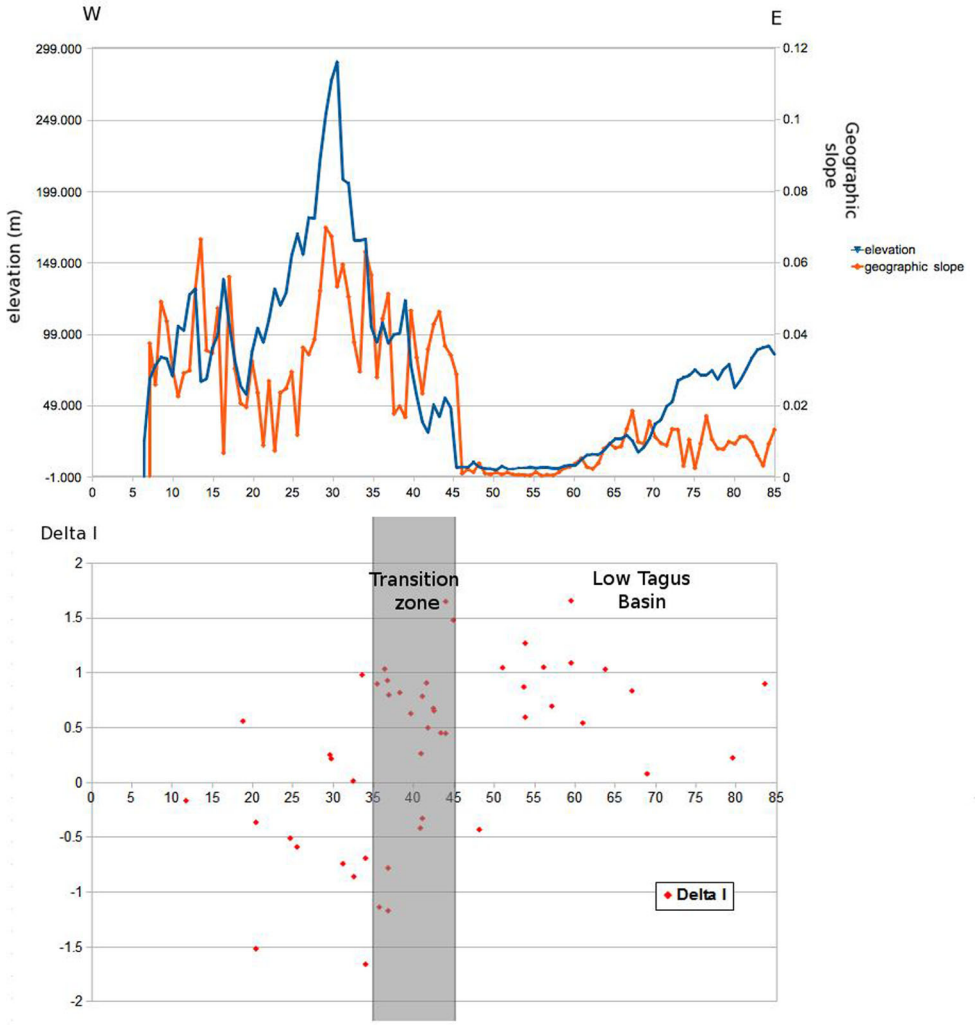

Figure 9. Relation between the geographic slope, the elevation and the intensity residuals. The orange curve represents the geographic slope along the profile. The blue curve represents the elevation along the profile. Red dots represent the intensity residuals.

the location of an intensity data is associated to the closest municipality. So, the calculated epicentral distance corresponds to the distance between the earthquake epicentre and this municipality, instead of the location of the observed intensity itself. According to the municipality density, this association may contribute to large uncertainties. Moreover, this intensity may be exaggerated if it results from a single testimony or a single damage statement.

Even if this attenuation laws present good results with the Bakun and Wentworth method (1997), or with the study of site effects, more steps of validations are required before using it into a Probabilistic Seismic Hazard Analysis. The attenuation law needs to be adapted according to different soil conditions. The map of residual intensities can be used to detect regions where site effect studies are suitable. Then, local site amplification effects will be accounted for by using empirical corrective coefficients.

Indeed, to use in PSHA calculation, the calculated intensities needs to be convert into spectral accelerations that may lead to largest uncertainties. After the intensity to acceleration conversion, the empirical accelerations need to be compared with accelerometer data.

7 CONCLUSION

A new method for computing attenuation law for the Portugal mainland has been presented in this paper. This method uses the intensity observations directly, rather than the areas enclosed by isoseismal lines, made up by subjective expert decisions. The significant advantage in using individual intensity observations directly is that the procedures are explicit so that the results are reproducible. Another improvement of this attenuation law is that it is expressed as a function of the magnitude.

From the logarithmic regression of each collected event and the study of their slope and intercept behaviour with the magnitude, we obtained the following attenuation law:

$$I = -1.9438 \ln(D) + 4.1 M_{\mathrm{w}} - 9.5763.$$

The range of validity corresponds to moment magnitude values between 4.4 and 6.2. So far this attenuation law may be used in Portugal mainland, but can be extend to a wider area by incorporating additional events of stable region (e.g. additional events from Spain to obtain an attenuation law for use in the Iberian Peninsula).

Using the new attenuation law with the methodology of Bakun & Wentworth (1997), we obtained better results in the 1909 Benavente earthquake epicentral position and magnitude estimation, than the use of the Atkinson & Boore (1997) attenuation law. We reached to a magnitude estimation of 6.1 for the 1909 Benavente event that is close to the instrumental one. This attenuation law does not consider the site effects. Comparing the intensity observations of the 1909 Benavente event to the ones computed with the attenuation, we can detect regions of amplification. The positive intensity residuals, considered as amplified intensities, match really well with the Meso-Cenozoic basins, known for their potential site effects. These local site amplification effects can be accounted for by using empirical corrective coefficient.

ACKNOWLEDGEMENTS

This research and Boris Le Goff are funded by the Fundação para a Ciência e a Tecnologia (FCT, Portugal) under the project SourceMod4PSHA – PTDC/CTE-GIX/102245/2008, FCOMP-01-0124-FEDER-009326. The authors acknowledge the funding provided by the Centro de Geofísica de Évora, Portugal, under the contract with the FCT, PEst-OE/CTE/UI0078/2011 and the project QuakeLoc-PT – PTDC/GEO-FIQ/3522/2012 (Portugal). We would also like to acknowledge Delphine Fitzenz for the support provided in the framework of project LTV-SourceMod4PSHA. We thank Óscar López López for his involvement in GIS map development with QGIS. This article benefited a lot from suggestions provided by anonymous reviewers.

REFERENCES

Ambraseys, N., Simpson, K. & Bommer, J., 1996. Prediction of horizontal response spectra in Europe, *Earthq. Eng. Struct. Dyn.,* **25,** 371–400.

Atkinson, G. & Boore, D., 1997. Some comparisons between recent ground motion relations, *Seismol. Res. Lett.,* **68,** 24–40.

Bakun, W.H. & Wentworth, C.M., 1997. Estimating earthquake location and magnitude from seismic intensity data, *Bull. seism. Soc. Am.,* **87,** 1502–1521

Bensaúde, A., 1910. Le tremblement de terre de la vallée du Tage du 23 avril 1909 (Note préliminaire), *Bull. Soc. Port. Sc. Nat.,* **3,** 89–129.

Bezzeghoud, M., Borges, J.F. & Caldeira, B., 2011. Ground motion Simulations of the SW Iberia Margin: rupture directivity and earth structure effects, *Nat. Hazard,* **69**(2), 1229–1245.

Borges, J.F., Fitas, A.J.S., Bezzeghoud, M. & Teves-Costa, P., 2001. Seismotectonics of Portugal and its adjacent Atlantic area, *Tectonophysics,* **337,** 373–387.

Buforn, E., Udias, A. & Colombas, A., 1988a. Seismicity, source mechanisms and tectonics of the Azores-Gibraltar Plate boundary, *Tectonophysics,* **152,** 89–118.

Buforn, E., Mézcua, J. & Udias, A., 1988b. Mecanismo focal del terramoto del Cabo San Vicente de 20 de Octubre de 1986, *Rev. Geofís.,* **44,** 109–112.

Buforn, E., Sanz de Galdeano, C. & Udias, A., 1995. Seismotectonics of the Ibero-Maghrebian region, *Tectonophysics,* **248,** 247–261.

Cabral, J., Moniz, C., Terrinha, P., Matias, L. & Ribeiro, P., 2000. Analysis of seismic reflection profiles in the neotectonic characterization of the Lower Tagus Valley area, in, *XXVII General Assembly of the European Seismological Commission,* Lisbon (Portugal), 10–15 September, SSC1-07-P, 72.

Cabral, J., Ribeiro, P., Figueiredo, P., Pimentel, N. & Martins, A., 2004. The Azambuja fault: an active structure located in an intraplate basin with significant seismicity (Lower Tagus Valley, Portugal), *J. Seismol.,* **8,** 347–362.

Choffat, P. & Bensaude, A., 1912. Estudos sobre o sismo do Ribatejo de 23 de Abril de 1909, Com. Serv. Geol. Port., Lisbon, p. 146.

Choi, Y., Stewart, J.P. & Graves, R.W., 2005. Empirical model for basin effects accounts for basin depth and source location, *Bull. seism. Soc. Am.,* **95**(4), 1412–1427.

Dineva, S., Batllo, J., Mihaylov, D. & Van Eck, T., 2002. Source parameters of four strong earthquakes in Bulgaria and Portugal at the beginning of the 20th century, *J. Seismol.,* **6,** 99–123.

Grandin, R., Borges, J.F., Bezzeghoud, M., Caldeira, B. & Carrilho, F., 2007. Simulations of strong ground motion in SW Iberia for the 1969 February 28 (Ms = 8.0) and the 1755 November 1 (M ∼ 8.5) earthquakes—I. Velocity model, *Geophys. J. Int.,* **171**(3), 1144–1161.

Johnston, A., 1996a. Seismic moment assessment of earthquakes in stable continental regions—I. Instrumental seismicity, *Geophys. J. Int.,* **124,** 381–414.

Kárník, V., 1969. *Seismicity of the European Area*, Part 1, Reidel.

López Casado, C., Delgado, J., Peláez, J.A., Peinado, M.A. & Chacón, J., 1992. Site effects during Andalusian earthquake (12/25/1884), in *Proceedings of the 10th WCEE,* Vol. **2,** pp. 1085–1089, ed. Madrid, A.A., Balkema.

López Casado, C., Molina Palacios, S., Delgado, J. & Peláez, J., 2000. Attenuation of intensity with epicentral distance in the Iberian Peninsula, *Bull. seism. Soc. Am.,* **90,** 34–47.

Martín, A.J., 1984. Riesgo Sísmico en la Península Ibérica, Tesis Doctoral, Talleres del Instituto Geográfico Nacional, Vols I and II (in Spanish).

Mezcua, J., 1982. *Catalogo general de isosistas de la Península Ibérica*, Instituto Geográfico Nacional.

Moreira, V.S., 1991. Historical seismicity and seismotectonics of the area situated between the Iberian Peninsula, Marrocco, Selvagens and Azores Islands, in *Seismicity, Seismotectonic and Seismic Risk of the Ibero-Magrebian Region,* Publicacion I.G.N. Série Monografia 8, pp. 213–225, Instituto Geográfico Nacional.

Muñoz, D., 1974. Curvas medias de variación de la intensidad sísmica con la distancia epicentral, *Tesis Licenc*. Fac. Cien. Físicas, Univ. Complutense, Madrid (in Spanish).

Paolucci, R. & Morstabilini, L., 2006. Non-dimensional site amplification functions for basin edge effects on seismic ground motion, in *Third International Symposium on the Effects of Surface Geology on Seismic Motion Grenoble,* France, 30 August–1 September 2006, Paper Number 41.

Senos, L., Ramalhete, D. & Taquelim, M.J., 1994. Estudo dos principais sismos que atingiram o território de Portugal Continental, Inst. Meteo., Lisbon, Monography 46.

Sousa, M.L. & Oliveira, C.S., 1997. Hazard mapping based on macroseismic data considering the influence of geological conditions, *Nat. Hazards,* **14,** 207–225.

Stich, D., Batllo, J., Macia, R., Teves-Costa, P. & Morales, J., 2005. Moment tensor inversion with single-component historical seismograms: the 1909 Benavente (Portugal) and Lambesc (France) earthquakes, *Geophys. J. Int.,* **162,** 850–858.

Teves-Costa, P. & Batlló, J., 2011. The 23 April 1909 Benavente earthquake (Portugal): macroseismic field revison, *J. Seismol.,* **15**(1), 59–70.

Teves-Costa, P., Borges, J.F., Rio, I., Ribeiro, R. & Marreiros, C., 1999. Source parameters of old earthquakes: semi-automatic digitization of analog records and seismic moment assessment, *Nat Hazarads,* **19,** 205–220.

Teves-Costa, P., Batlló, J., Rio, I. & Macià, R., 2005. O sismo de Benavente de 23 de Abril de 1909—Estado da arte, in *Proceedings of the 4° Simpósio de Meteorologia e Geofísica da APMG*, Sesimbra, 14–17 February, pp. 44–49.

Toro, G.R., Abrahamson, N.A. & Schneider, J.F., 1997. Model of strong ground motion from earthquakes in central and eastern North America: best estimates and uncertainties, *Seismol. Res. Lett.,* **68**(1), 41–57.

Vilanova, S.P. & Fonseca, J.F.B.D., 2007. Probabilistic seismic-hazard assessment for Portugal, *Bull. seism. Soc. Am.,* **97,** 1702–1717.